Cross-Discipline Integration in Reservoir Modeling: The Impact on Fluid Flow Simulation and Reservoir Management

Hisham M. Al-Qassab,
Mohammed A. Al-Khalifa,
Gurhan Aktas
John Fitzmaurice,
Zaki A. Al-Ali, and
Paul W. Glover

Al-Qassab is the team leader of the Northern Onshore and Central Arabia Team of Reservoir Characterization Department. He is a PhD candidate and holds a bachelor's degree in geology from the University of Alabama and a master's degree from King Fahd University of Petroleum and Minerals (KFUPM). His work focuses on data integration in reservoir modeling. Al-Khalifa is a geological modeler working with the Northern Onshore and Central Arabia Team of Reservoir Characterization Department. He holds a bachelor's degree in geology from KFUPM and is working on his master's degree at KFUPM. Al-Khalifa is a member of the American Association of Petroleum Geologists (AAPG). Aktas joined Saudi Aramco's Reservoir Characterization Department in 1993. He previously was with Robertson Research, U.K., and EIE of Turkey. He has a BSc in geological engineering from Istanbul University, an MSc from Leeds University and a PhD from Edinburgh University, U.K. His interests include sequence stratigraphy, sedimentology and reservoir characterization of both clastic and carbonate reservoirs. He is a member of the AAPG and the London Geological Society. Fitzmaurice received a BSc in geophysics in 1978 from Virginia Tech in Blacksburg, Virginia. He worked at Texaco from 1978 to 1985 and then joined Saudi Aramco. He is a member of the Society of Exploration Geologists, AAPG and European Association of Geoscientists and Engineers. Al-Ali joined the Saudi Ministry of Petroleum and Minerals Resources after receiving his BS in petroleum engineering from KFUPM in 1983. In 1987 he obtained an MS degree in petroleum engineering from KFUPM and joined Saudi Aramco. Al-Ali has worked in several petroleum industry sectors including production, drilling and reservoir engineering. He contributed to the development of new correlations and methods of cost savings.

ABSTRACT

A new technique has been developed for modeling 3D permeability distributions. The technique integrates all available data into a fluid flow simulation model. The integrated modeling process honors the essential aspects of the established reservoir descriptions as well as geological facies models and engineering data.

The added value of data integration of the fluid flow simulation is illustrated by the improved accuracy of the resulting well performance predictions and the decrease in time requirements for reservoir modeling history matching.

The technique utilizes diverse data at different scales to condition reservoir models of facies, porosity and permeability. Such data includes 3D seismic, well logs, core measurements, geologic facies distribution, flow meter logs and pressure buildup tests. The model building process explicitly accounts for the difference in scale of the various measurements. The model calculates the porosity, facies and permeability in the inter-well volume using geostatistical techniques that are constrained by seismic impedance derived from 3D seismic data. The use of engineering data in the permeability modeling constrains the results and decreases the history matching time requirements.

A case study demonstrates the modeling technique. A reservoir model is developed for the 'Unayzah formation in the Hawtah field of Saudi Arabia. The 'Unayzah is a highly stratified clastic reservoir in a mixed fluvial and eolian depositional environment. Data integration provided a more realistic reservoir model for this complex geologic setting than the conventional approach. Specifically, the integrated approach provided a reservoir model that captured the complex and highly stratified nature of the lithological units. Fluid flow simulation was carried out for both the new integrated reservoir model and the conventional reservoir model. Results show tremendous savings in history matching time and more accurate results for use in reservoir management production strategies when applying the new technique.

INTRODUCTION

At present there is an increasing demand for detailed geological numerical models, which incorporate all available data into reservoir characterization studies for the purpose of fluid flow simulation. Conventional modeling techniques, which lack the ability to quantitatively integrate data, tend to produce homogenous results of reservoir properties in the inter-well regions.

These models, when fed into reservoir simulations for performance predictions, may generate biased and unreliable results. This necessitates the development of a method that integrates all available data, despite differences in scale, improving the predictive power of the models and making it possible to obtain quicker production history matching from reservoir simulation.

One of the primary reasons for using geostatistics in the reservoir modeling process is data integration. That is, it allows the incorporation of diverse data of varying scale. This can include very descriptive data, such as conceptual geologic interpretations, or measurements such as 3D seismic time traces, their derivatives and the resulting interpretations. Geostatistical tools can use data such as 3D seismic to directly or indirectly contribute to the modeling of the inter-well regions. This may provide significant risk reduction in reservoir development and management.

This paper presents a geostatistical methodology that has been adopted for integrating geophysical, geological and engineering data in reservoir modeling. The Hawtah field, located in the central part of Saudi Arabia (fig. 1), has been chosen to demonstrate the approach. Hawtah is a recently developed field with a wealth of modern geological, petrophysical, geophysical and production data. Incorporating all of this information into the reservoir model exceeded the capability of conventional numerical models.

Depositional facies maps representing geologic environments were generated using core-calibrated electrofacies from well logs. The facies model was generated by geostatistical interpolation of the electrofacies logs using Sequential Indicator Simulation (SIS).

A stochastic seismic post-stack amplitude inversion was carried out to produce a high-resolution (well log scale) acoustic impedance model. A porosity model was then generated using both the SIS facies model and the acoustic impedance model as soft data. Finally, a permeability model was constructed, which is conditioned to Kh from pressure buildups allocated by flow meter profiles, core data and the resulting porosity model.

Reservoir properties of this integrated model were then input to the reservoir simulation and the history match results

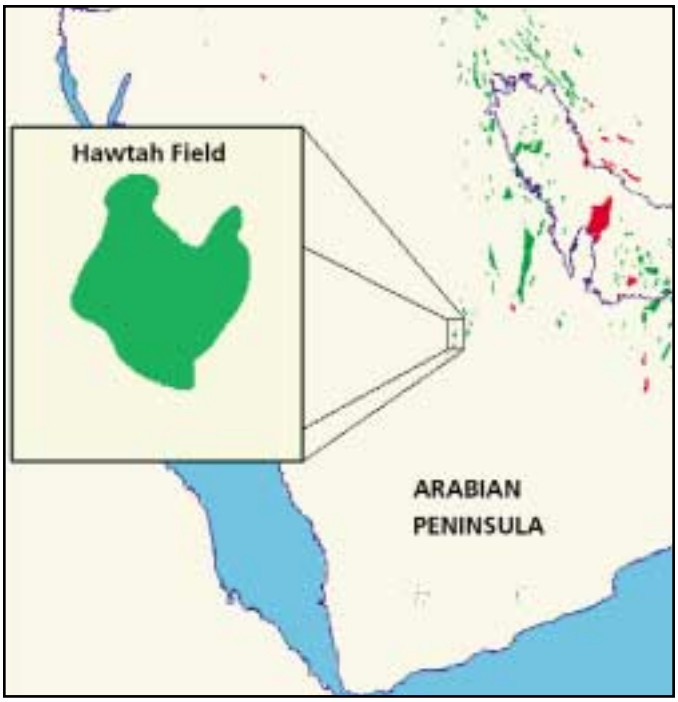

Fig. 1. Location map of Hawtah field

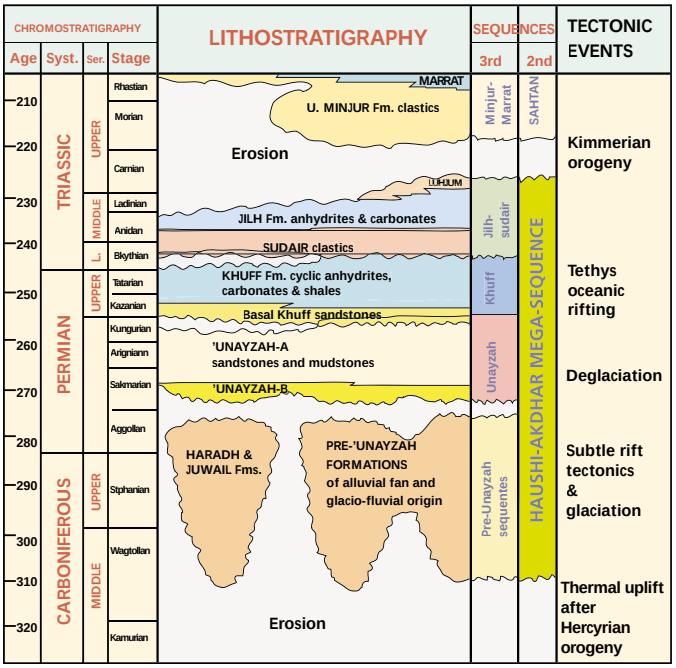

Fig. 2. 'Unayzah stratigraphic chart

compared with those of the conventional models. Histograms of pressure match, CPU versus time steps and error analysis plots are displayed for comparative analysis for flow predictions using both models.

STRATIGRAPHIC AND RESERVOIR ARCHITECTURE OF 'UNAYZAH RESERVOIRS IN HAWTAH FIELD

The 'Unayzah reservoirs in the Hawtah field are composed largely of rocks of continental origin, organized in a highly complex fashion. Untangling the complex facies architecture of these reservoirs has required passing through several evolutionary stages. Earlier conceptions advocated a complex picture with a relatively random distribution of reservoir and non-reservoir facies distributions. However, more recent detailed stratigraphic and sedimentological studies suggest that the rock architecture of the 'Unayzah reservoirs is in fact much better organized than originally believed. Furthermore, a sequence stratigraphic scheme can be applied to allow a better understanding of reservoir prediction and connectivity for most parts of the reservoirs.

The 'Unayzah reservoirs in the Hawtah field can be divided into three major units: the basal Lower 'Unayzah (B), the middle Upper 'Unayzah (A), and locally well-developed basal Khuff clastics on top (fig. 2).

The Lower 'Unayzah (B) and underlying pre-'Unayzah sequences represent sedimentary successions filling a structurally irregular topography (post orogenic early rift) following the Hercynian orogeny. These sediments are composed of dry and wet alluvial fan and also associated glaciofluvial deposits.

The sediments of 'Unayzah (A) signal a major shift in depositional and tectonic styles from underlying 'Unayzah (B) sandstones. The principal reservoir unit of the 'Unayzah (A) can be divided into five major aggradational cycles which are laterally correlatable and can be further subdivided into 13 sequences. Individual cycles show upward-cleaning characteristics, most commonly starting with trangressive lacustrine and associated sabkha and interdune facies in the lower parts, followed by aeolian, and locally by ephemeral fluvial channel deposits in variable proportions. These cycles represent overall upward-drying sequences developed in response to fluctuating climatic conditions probably caused by large-scale cyclic orbital variations. Lake transgressions are attributed to the periods of deglaciation of gradually diminishing icecaps. Thickening of cycles along the flanks of fields is attributed to ongoing subtle differential tectonic subsidence.

The youngest reservoir unit, the Basal Khuff, is characterized in the study area by localized lowstand incised valley fill sandstones, which form locally prominent high-quality reservoir bodies.

This brings the total number of stratigraphic sequences/zones to 15, which will be used for the purpose of reservoir modeling.

'UNAYZAH DEPOSITIONAL FACIES MAPS AND MODEL

The goal of building facies models in any reservoir characterization study is to identify the spatial distribution of rock types that control fluid flow behavior. However, one difficulty in any study, including this one, is the availability and quality of core data that define rock or facies types. Therefore, we adopted a two-fold method.

First, we identify facies types and associations in terms of depositional environment from cored wells so that geological characteristics can be explained in details that are geologically

TABLE 1. DESCRIPTION OF DEPOSITIONAL ENVIRONMENTAL FACIES

FACIES TYPE	DESCRIPTION
Dune	Medium to fine grained clean sandstones, well sorted, poorly cemented.
Interdune	Very fine to fine grained, moderately argillaceous sandstones, horizontal to wavy laminated.
Lake margin sabkha	Very fine grained sandstone, interlaminated with silty layers. Horizontal to wavy bedded.
Fluvial	Fine to coarse grained, poorly sorted sandstones, organized into sharp erosive based upward-fining package.
Lacustrine	Variable silty mudstones, present in varying thicknesses, most commonly at the base of upward-drying cycles.

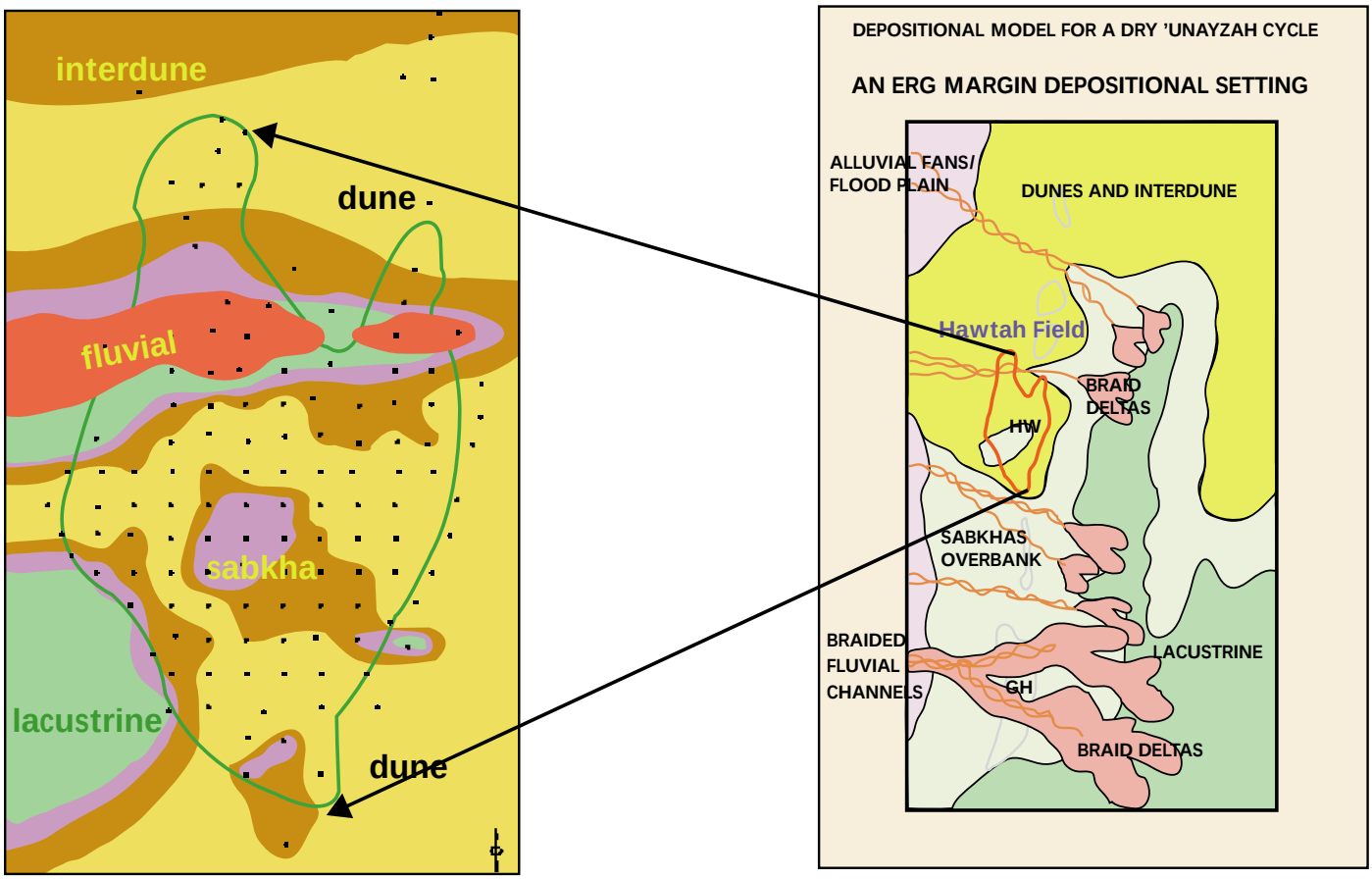

Fig. 3. Hand-contoured map (left) of depositional facies using well data and regional depositional setting (right)

sound. Once the facies were identified at cored wells, they were extended to non-cored wells, which have well logs available. The output from this method was a foot-by-foot determination of depositional environmental facies types in each well in Hawtah field. Table 1 shows a description of each of the depositional environmental facies associations.

Facies maps were hand-drawn by the geologist for each of the 13 zones within 'Unayzah (A) reservoir. This was accomplished by simply assigning a facies type for each well for a given zone. This facies type represents the facies with the highest proportion for a given zone. A facies value was then plotted for every well location, and directional data from bore hole image logs in the form of a trend were placed next to the facies type. This map was then hand-contoured honoring the facies type, directional indication from well image logs and the regional depositional characteristics of 'Unayzah formation (fig. 3).

These hand-drawn maps were then used to build a 3D environment of depositional facies model for the entire reservoir. This was done by treating each facies type from the hand-drawn facies maps as a region, and then separately distributing facies available at wells within that region using a categorical geostatistical algorithm for facies, namely SIS. Fig. 4 shows comparisons between facies maps for a selected zone and the resulting 3D model.

'Unayzah petrophysical rock model

Examination of reservoir properties such as porosity and permeability for their different depositional environmental facies indicated substantial overlap between them, as clearly seen in fig. 5. Therefore, it was concluded that depositional environmental facies could not be used alone to determine reservoir flow units for the purpose of this study. As a result, an in-house cluster analysis was used to establish petrophysical rock types for all the wells utilizing eight electric log curves. These petrophysical rock types were then cross-referenced with the core data.

The result showed three main petrophysical rock types with a distinct reservoir quality for each one: namely reservoir-rock (rock 1), an intermediate rock type (rock 2), and non-reservoir rock (rock 3). Table 2 shows detailed descriptions of each rock type. Furthermore, univariate

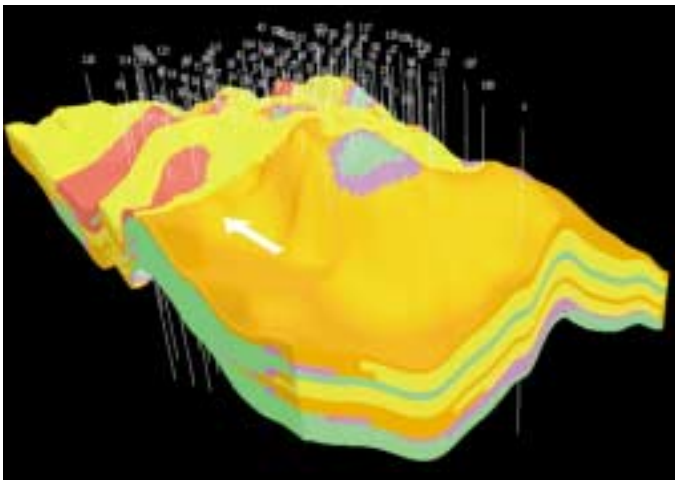

Fig. 4a. Stacked depositional environmental facies maps for the 13-zones

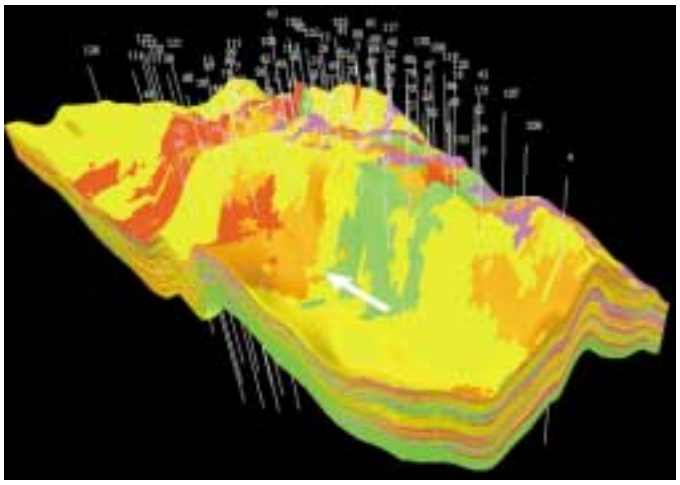

Fig. 4b. 3D model of depositional environmental facies

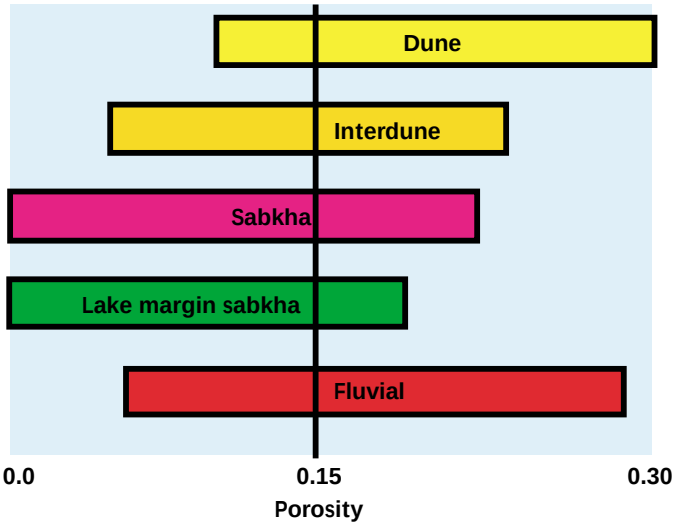

Fig. 5. Porosity ranges of depositional environmental facies

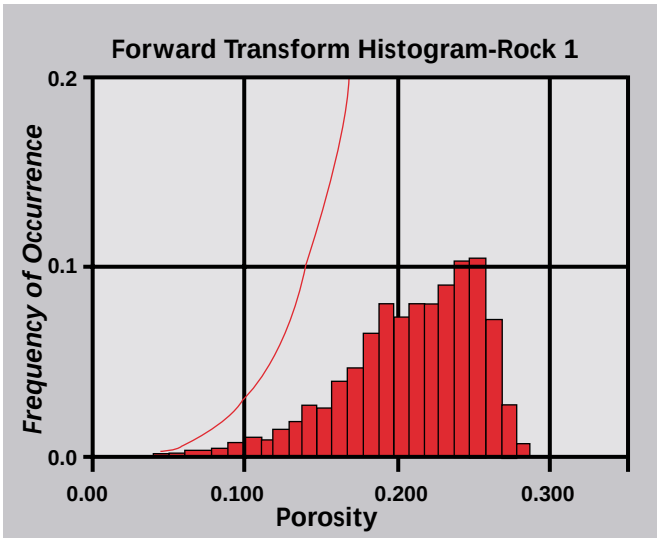

Fig. 6a. Porosity distribution of petrophysical rock 1 type

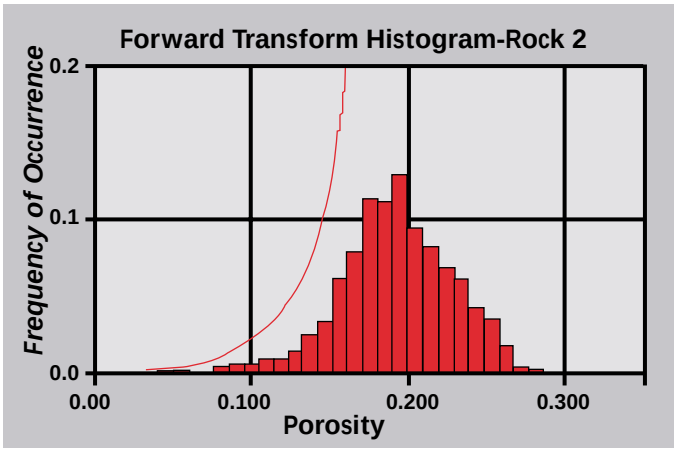

Fig. 6b. Porosity distribution of petrophysical rock 2 type

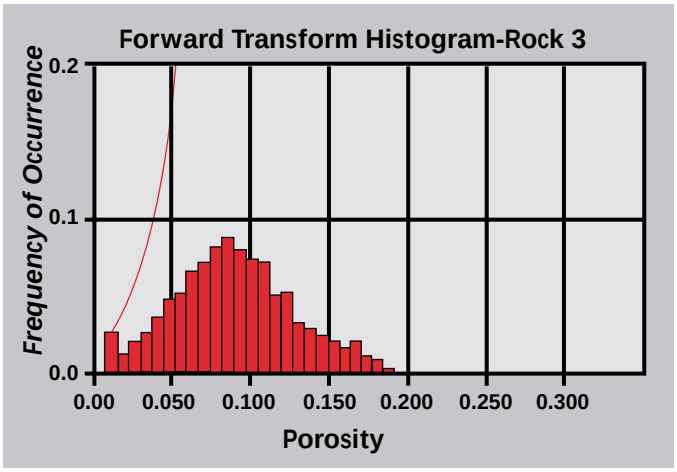

Fig. 6c. Porosity distribution of petrophysical rock 3 type

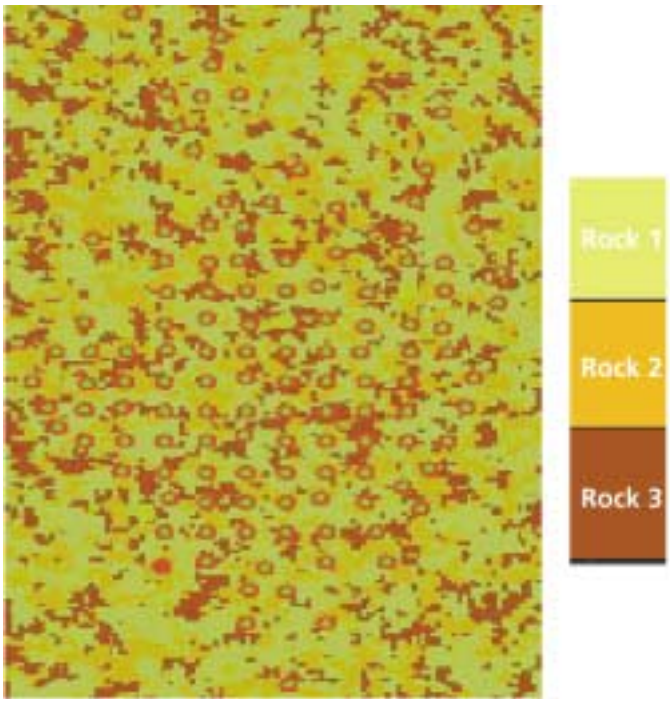

Fig. 7. Slice of the petrophysical rock model

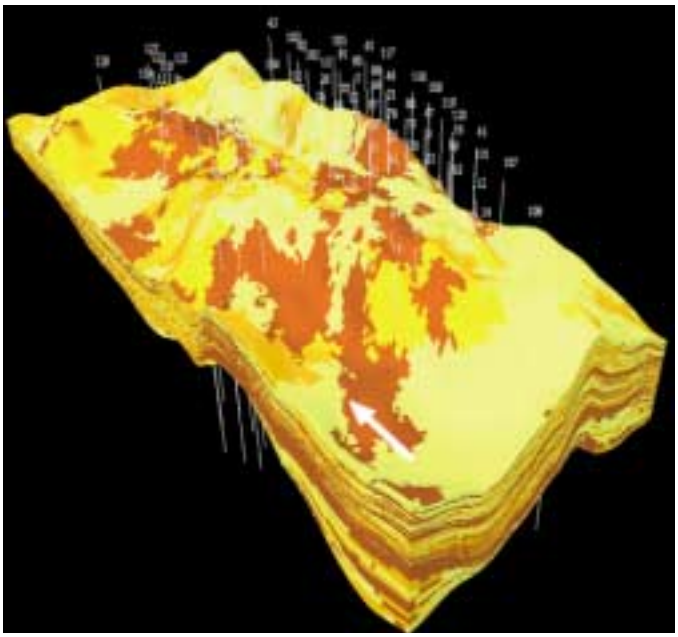

Fig. 8. Petrophysical rock model using rock types defined at wells and environment of depositional facies model as regions

statistics of porosity for each rock type show clear separation between each class of porosity as indicated in the histograms shown in fig. 6.

An attempt was made to build a 3D petrophysical rock model as defined at the wells, but the resulting model (fig. 7) has no geological character or meaning. Therefore, it was decided to combine both the environmental/depositional facies model built earlier, fully supported by the geologist, with the petrophysical rock type model, supported by the reservoir engineer, into a single integrated facies model. This was accomplished by distributing the petrophysical rock types defined at the wells within each environment of depositional facies separately. Fig 8 shows the resulting 3D model of petrophysical rock type distributions utilizing a depositional environmental facies model as regions.

Stochastic seismic inversion

A post-stack amplitude inversion was performed on the 3D Hawtah seismic volume for the purpose of incorporating seismic impedance data into the 3D Hawtah model. That is, the available seismic data was transformed from wiggle trace information to acoustic impedance to be useful for influencing 3D reservoir descriptions. This transformation and integration explicitly considered that seismic-based information is an imperfect predictor of well impedance logs and, subsequently, an even less perfect predictor of facies.

Stochastic inversion has been employed in this study in place of the conventional deterministic approach, which gives absolute impedance results with resolution dependent on the inherent seismic bandwidth. The stochastic inversion approach capitalizes on stochastic simulations such as Sequential Gaussian Simulation (sGs)-including collocated cokriging to generate multiple, equi-probable realizations of impedance pseudo-logs at each seismic trace location and then selecting the closest one to the actual seismic trace. Moreover, the stochastic inversion approach honors the constraining well impedance logs along with their vertical resolution as well as the specified univariate and bivariate statistics of impedance by area and/or zone.

Elements of the inversion processing of the 'Unayzah reservoir included a simultaneous wavelet estimation and time-depth analysis, zero-phase broadband reflectivity processing, 3D forward modeling of low-frequency reflectivity balancing and impedance fields, deterministic inversion, and a high-frequency log-scale stochastic simulation of impedance constrained by the deterministic inversion. The result is an impedance model at the same scale of resolution as the well logs as shown in fig 9.

TABLE 2. DESCRIPTION OF PETROPHYSICAL ROCK TYPES

ROCK TYPE	DESCRIPTION
Rock 1	Well sorted, medium to coarse grain sandstone. Connate water saturation of less than 10 percent and gamma ray of less than 30 API units.
Rock 2	Fine to medium grained silt sandstone. Gamma ray between 30-45 API units.
Rock 3	Fine grained siltstone. Gamma ray greater than 45 API units with high connate water saturation.

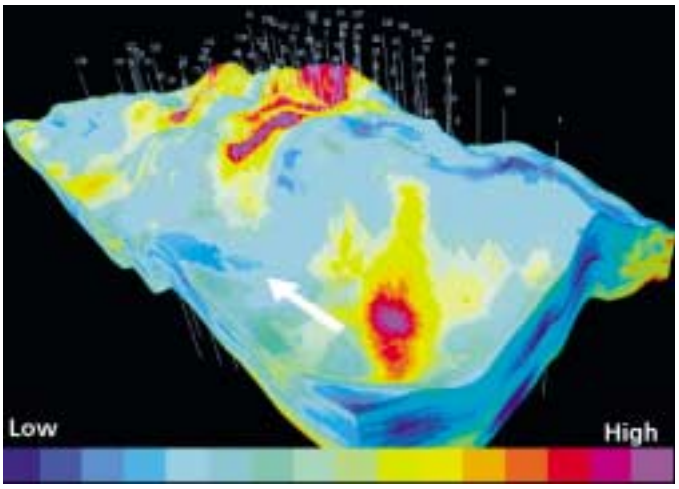

Fig. 9. High-resolution seismic impedance model as a product of stochastic inversion

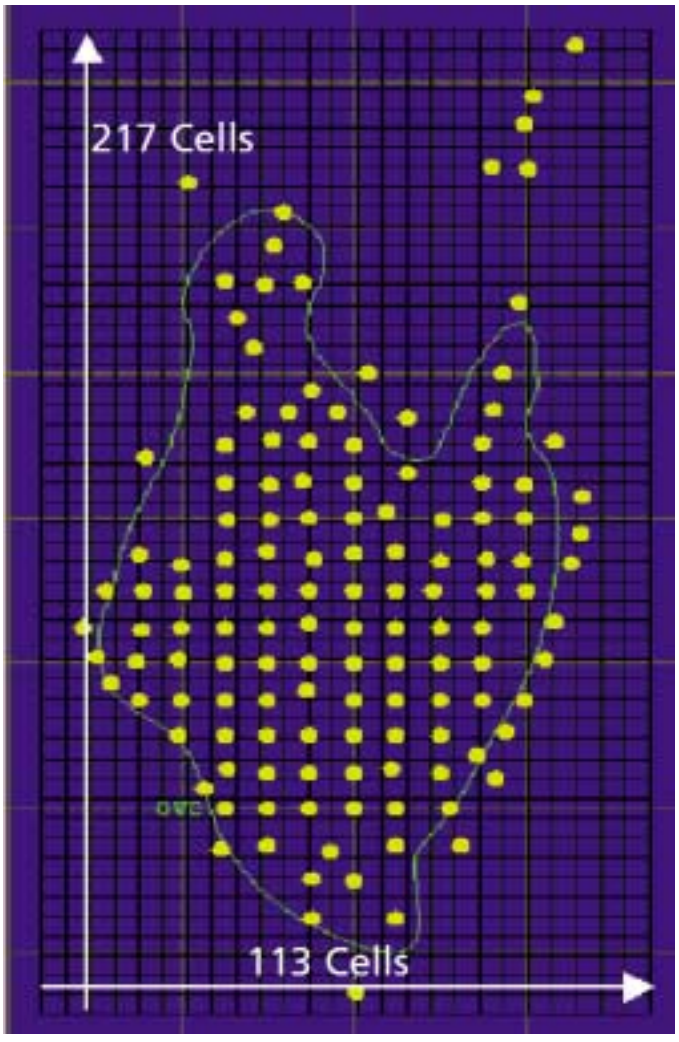

Fig. 10. Areal grid showing number of cells in X- and Y-directions

A seismic horizon picked at the top reservoir, combined with time-to-depth relationships determined from log-to-seismic-ties, was used to convert the geologic model layering scheme to seismic micro-horizons within the reservoir, and to estimate the seismic wavelet.

Time-to-depth conversion of Acoustic Impedance (AI)

Reservoir modeling is carried out in the depth domain, which requires the conversion of seismic acoustic impedance (AI) from the time-to-depth domain. The conversion can be done by simply snapping the impedance values between two markers, which are equivalent to the same depth markers, into a pre-defined 3D grid.

In the case of the 'Unayzah model, the geological 3D reservoir grid model was defined in depths utilizing all the 13 zones and an areal grid which covers the field outline. The total number of vertical cells (layers) is 133 with an areal grid of 113 in the x direction and 217 in the y direction (fig. 10), making the model size more than three million cells in total. AI data among each of the 15 zones (which are available in time domain) were snapped to the corresponding 15 zones in depth. This conversion from one domain to another is considered as an implicit one, unlike the conventional velocity-based conversion. Fig. 11 shows a schematic diagram of how this was done.

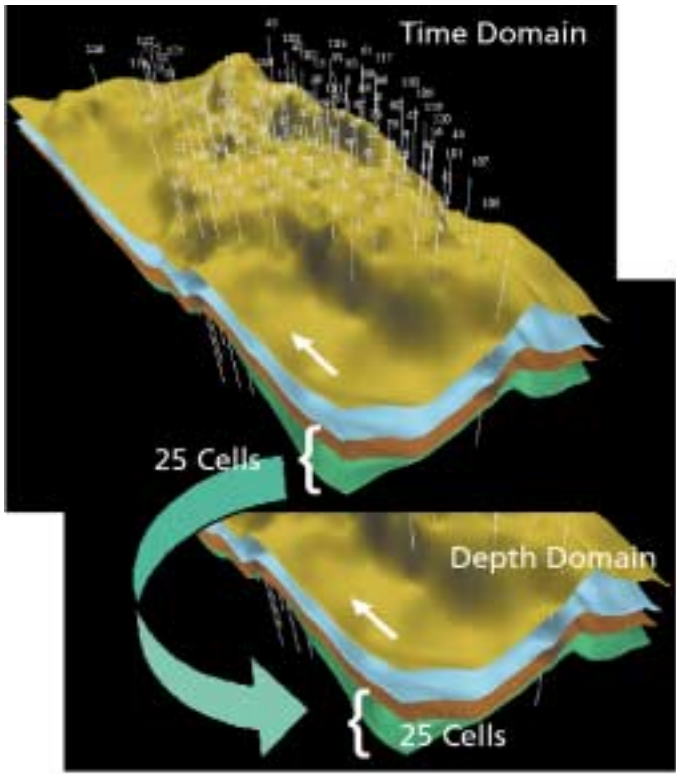

Fig. 11. Schematic diagram showing time, top, to depth, bottom and conversion. The 25 cells are snapped between two equivalent markers.

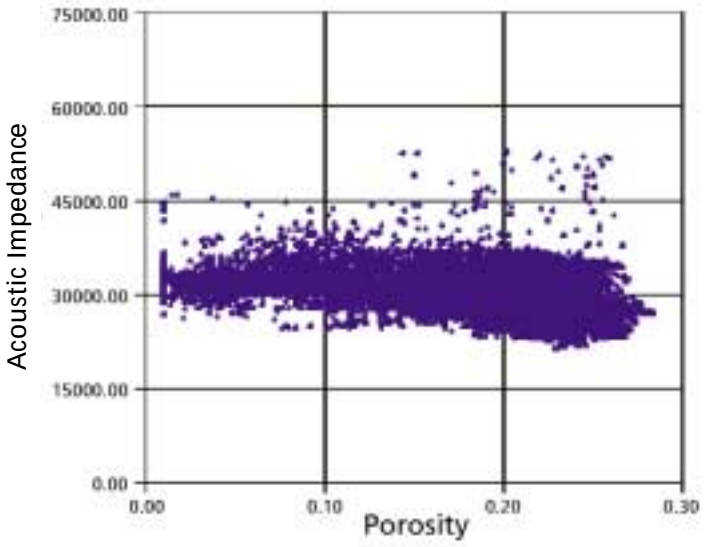

Fig. 12. Cross plot of well porosity, X-axis, AI and Y-axis, for the entire reservoir

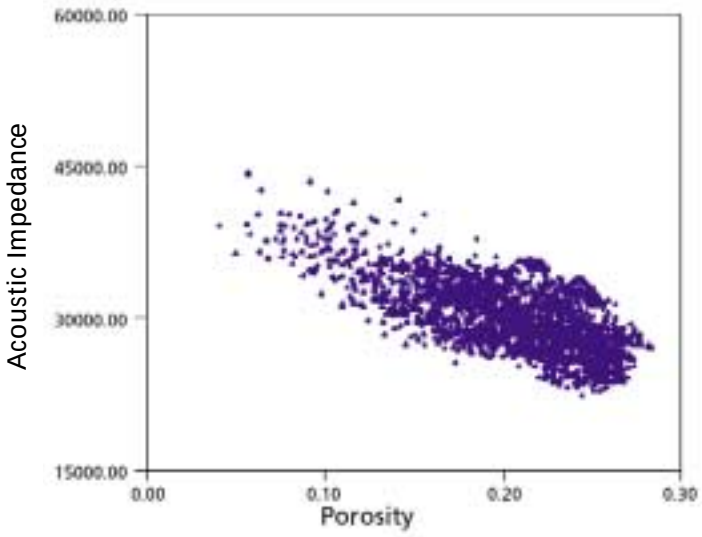

Fig. 13a. Cross plot of well porosity, X-axis, AI and Y-axis, for type 1 rock

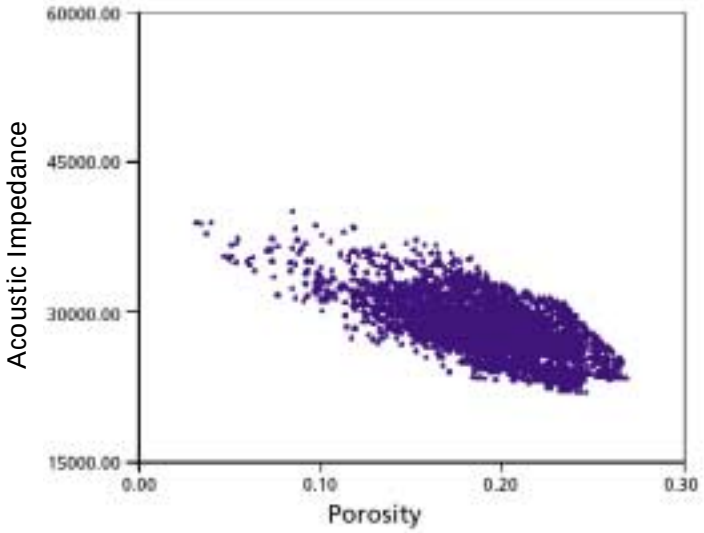

Fig. 13b. Cross plot of well porosity, X-axis, AI and Y-axis, for type 2 rock

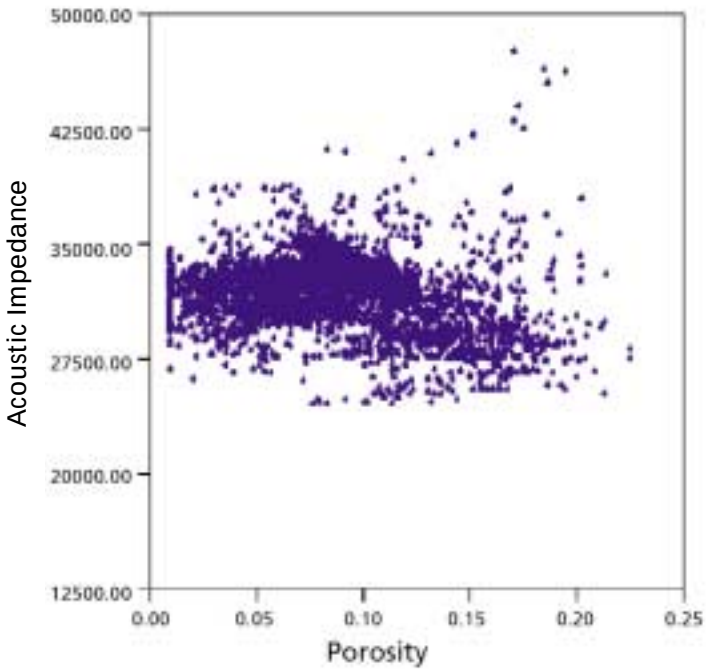

Fig. 13c. Cross plot of well porosity, X-axis, AI and Y-axis, for type 3 rock

Acoustic Impedance porosity relationship

Well data were thoroughly examined by means of univariate and bivariate analysis such as histograms and scattergrams, respectively, to look for a systematic relationship between well AI and porosity. Fig 12 shows a cross plot of porosity and AI, which indicated a large cloud of data with no strong relationship between these two variables. However, there was evidence of a strong AI and porosity relationship once the data was segregated by petrophysical rock type as shown in fig. 13. This figure shows that the better the reservoir quality rock (rock 1) the higher the correlation coefficient between porosity and AI. However, in the non-reservoir rock type (rock 3), the relationship between the two variables is lost. As a result, facies modeling plays a major role in determining how much weight the seismic should have to influence the estimation of porosity in the inter well regions.

Porosity and permeability modeling

A 3D porosity model was built using the high-resolution impedance model and utilizing the proper correlation coefficient for each rock type as defined in the 3D petrophysical rock model built earlier. This was accomplished through the use of sGs of porosity with collocated cokriging using AI as

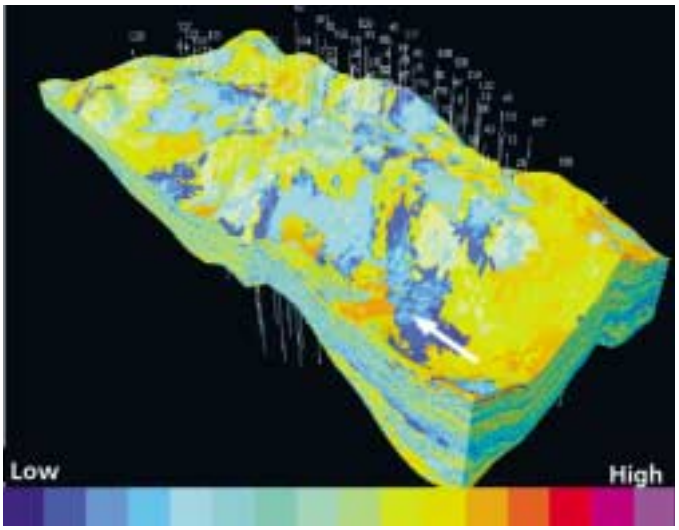

Fig. 14. Rock specific porosity model using sGs with collocated cokriging

soft data. Fig. 14 shows the resulting 3D model of facies' specific porosity. The sGs was chosen for its ability to generate models of porosity, which capture the heterogeneity of the reservoir as well as its power to generate multiple realizations of modeled porosity models, which can be ranked for use with fluid flow simulation tools, such as streamline simulation. In the case of 'Unayzah reservoir, only one realization of porosity was selected for fluid flow simulation for practical reasons.

Permeability curves were constructed for each well in the Hawtah field honoring both the permeability thickness from pressure buildups, flow meter profiles and core permeability data. The flow profile is used to allocate the total or gross measurement of pressure buildup to a higher resolution permeability log. Fig. 15 illustrates how flow meter data is used in allocating permeability logs which have the same scale and resolution as the flow meter profile. The newly produced permeability log is then integrated with core porosity and permeability data (fig. 16) for each facies to overcome the problem

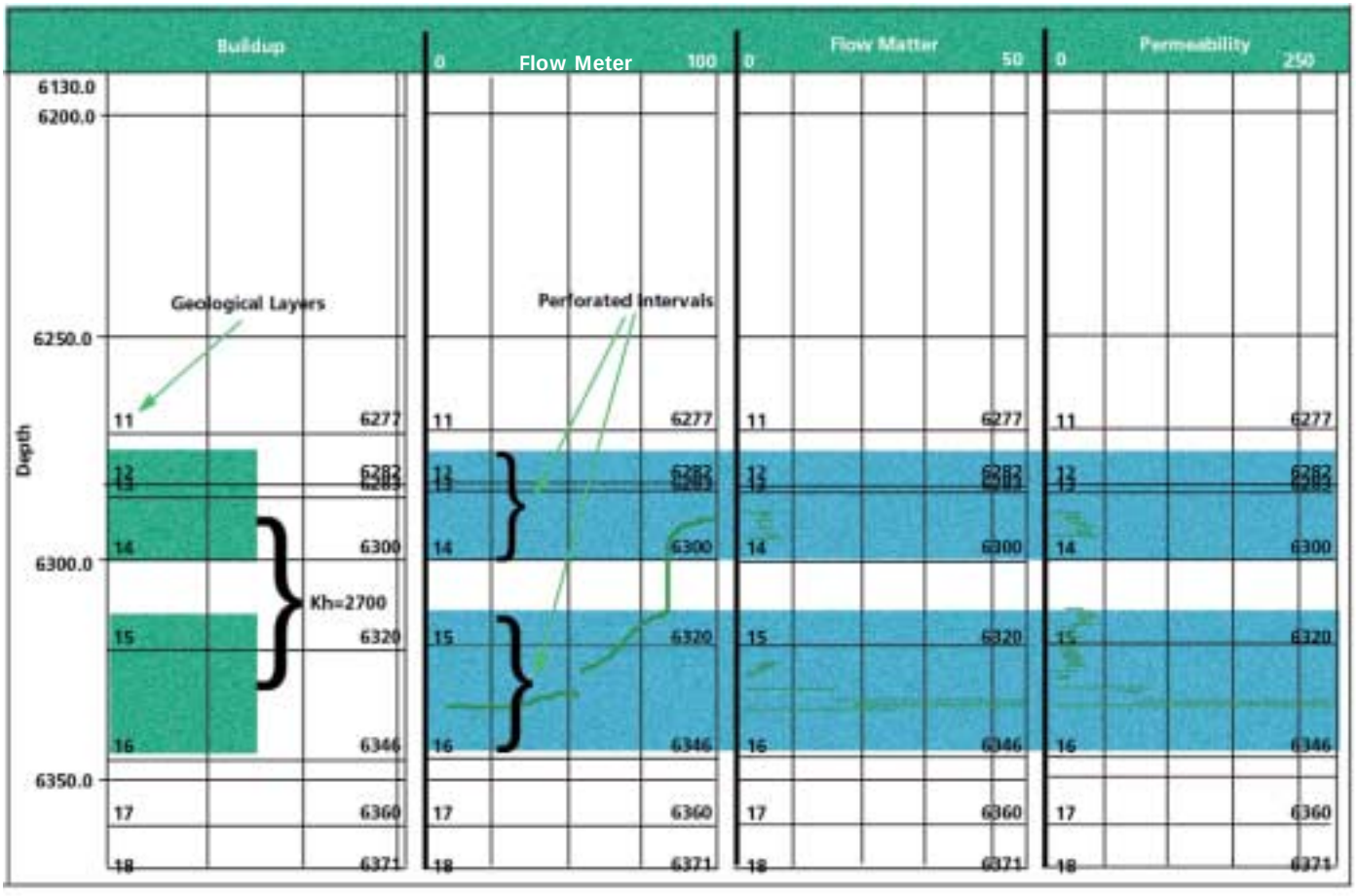

Fig. 15. Permeability thickness (Kh) allocated by flow meter profile in one of Hawtah field wells

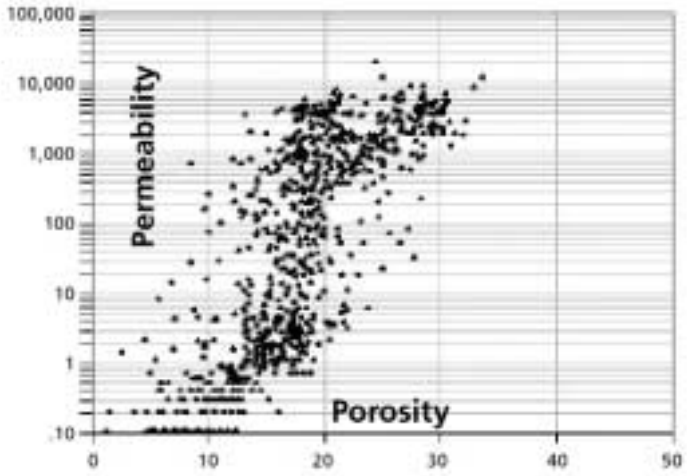

Fig. 16a. Cross plot of core porosity and permeability for type 1 petrophysical rock

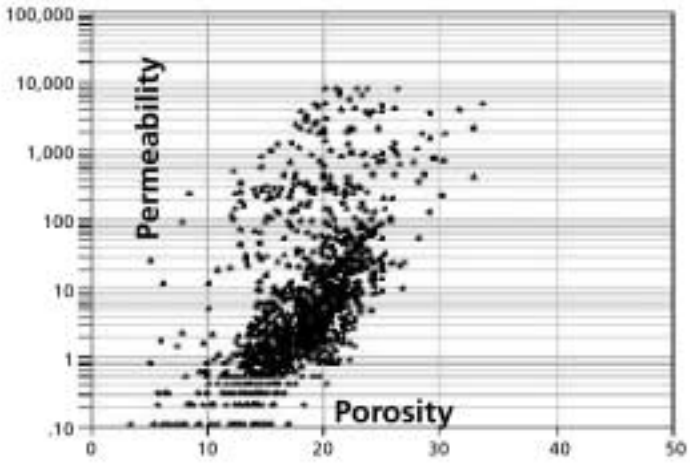

Fig. 16b. Cross plot of core porosity and permeability for type 2 petrophysical rock

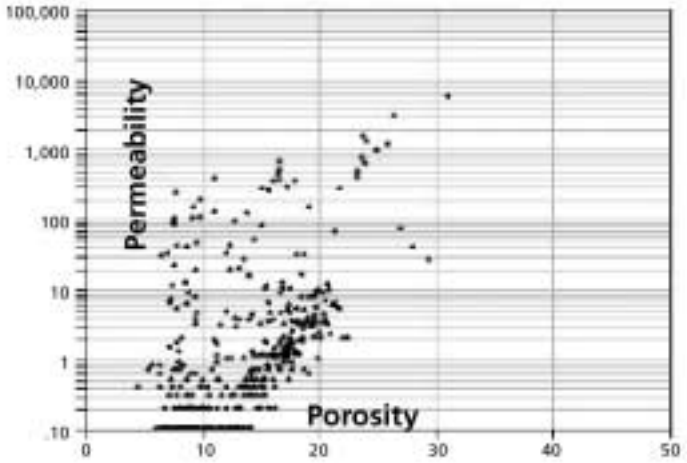

Fig. 16c. Cross plot of core porosity and permeability for type 3 petrophysical rock

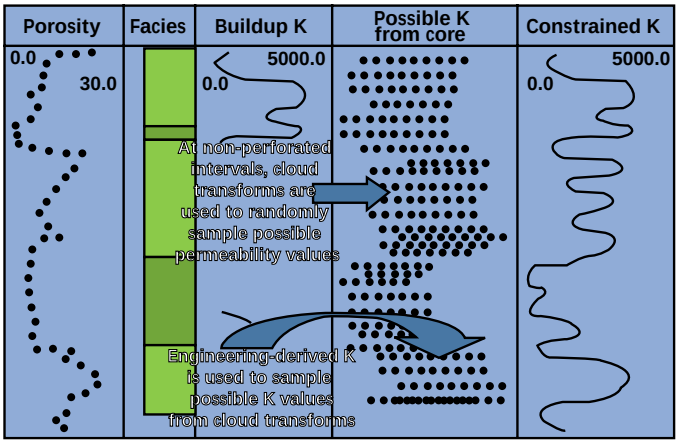

Fig. 17. Integrating buildup permeability as selecting criteria in sampling a range of permeability values from core data

of missing data at non-perforated intervals of the well. The integration is accomplished by assigning permeability values from cloud transforms of core porosity and permeability as shown in fig. 17.

In non-perforated intervals, however, facies-based cloud transforms are used to randomly sample possible permeability values from the core data for a given porosity class. A 3D correlated probability field was generated from the existing conditioned permeability logs at each well location. The correlated probability field is then used to sample the cloud transforms for each facies. For a given porosity value corresponding to the existing facies-based porosity model it then assigns a permeability value. The result is a permeability model that both honors the engineering data at the well location (permeability from pressure buildup and flow meter) and retains core porosity and permeability characteristics for each facies. Stratification of the 'Unayzah reservoir is better captured this way than using conventional techniques, as illustrated in fig. 18, where thin layers of high permeability are retained in the model that would have otherwise been lost.

Conventional porosity and permeability models

Two sets of porosity and permeability models were constructed using the interpolation methods of least squares and inverse distance and a linear transformation of porosity to permeability. Porosity was distributed between the wells using the inverse distance for the same 3D gridded integrated framework. Fig. 19 shows the inverse distance porosity model. This

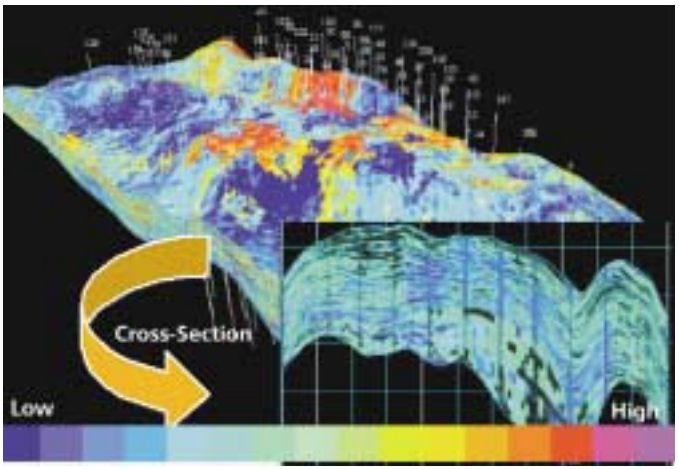

Fig. 18. 3D permeability model using core, engineering and seismically constrained rock-specific porosity model

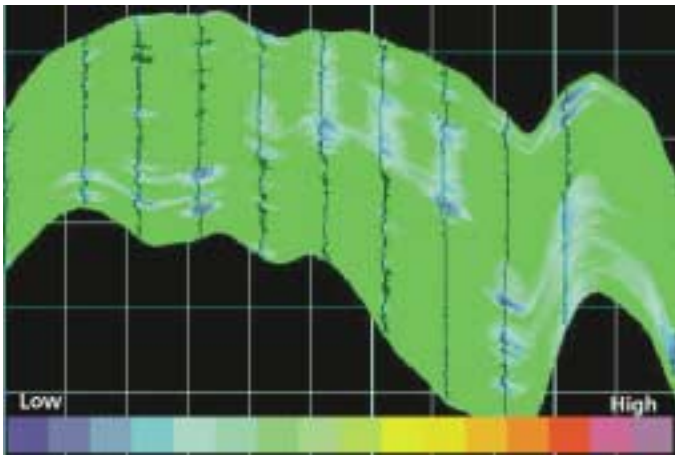

Fig. 19. Porosity model using inverse distance approach

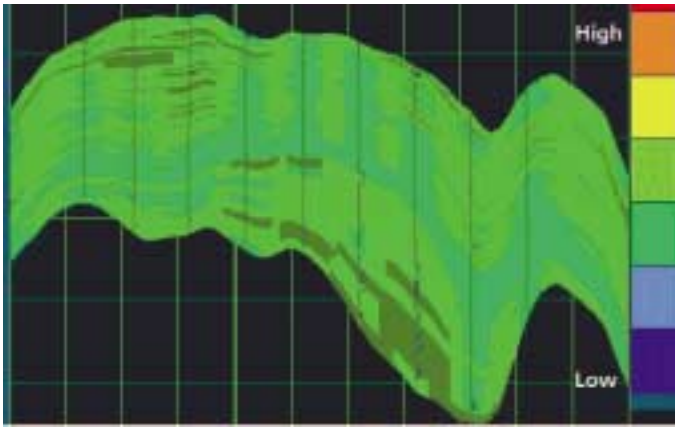

Fig. 20. Permeability model using linear transformation of porosity to permeability

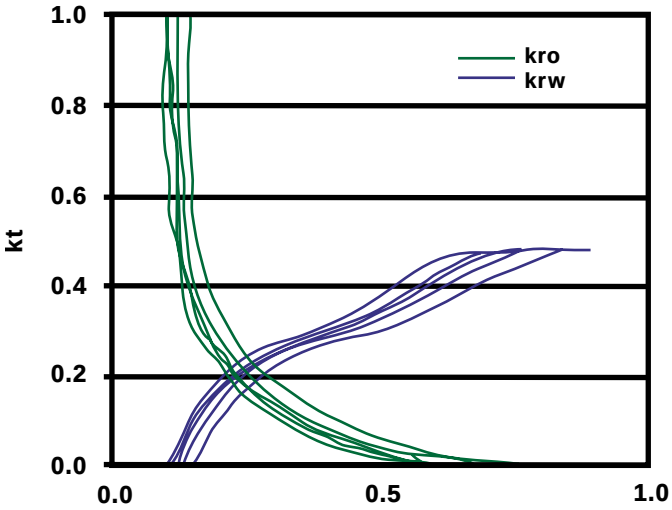

Fig. 21. An example of relative permeability curves for rock 1 tType with five porosity bins

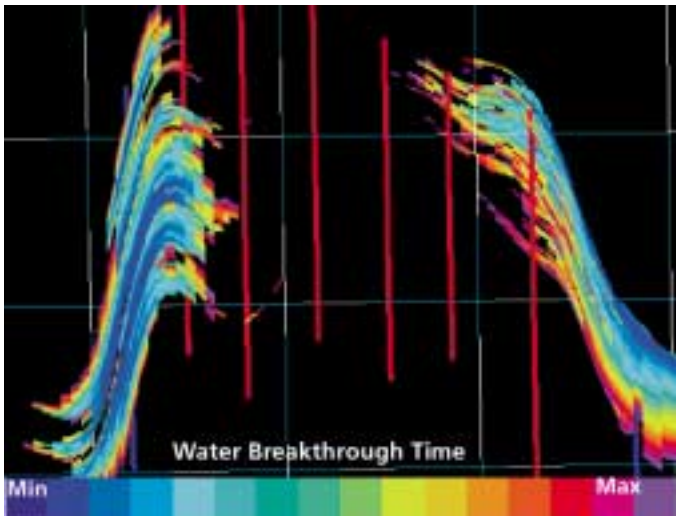

Fig. 22. Cross section of integrated model showing water breakthrough time. Note the stratification, right, of the reservoir.

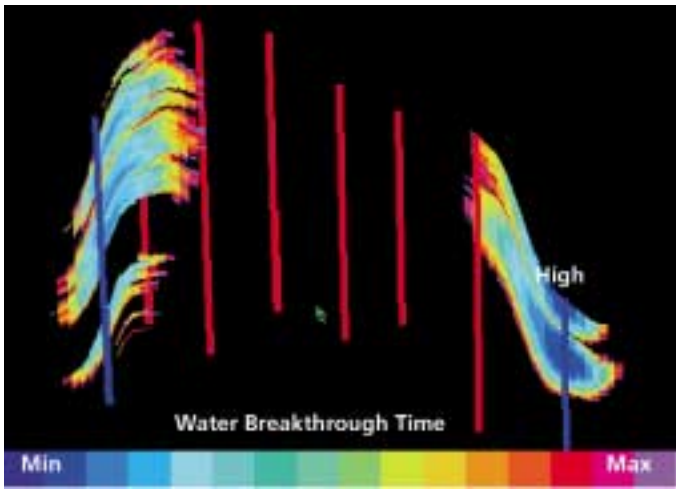

Fig. 23. A cross section of conventional model showing water breakthrough time. Note the uniform fluid front, right, of the reservoir.

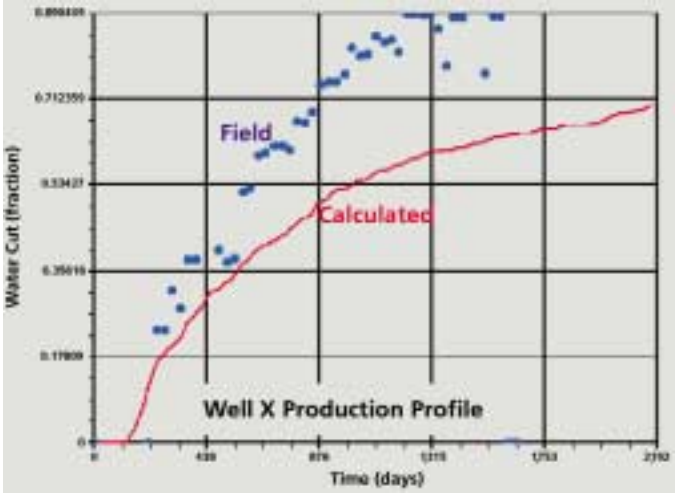

Fig. 24a. Water cut of integrated model. Note the water arrival time compared to field date.

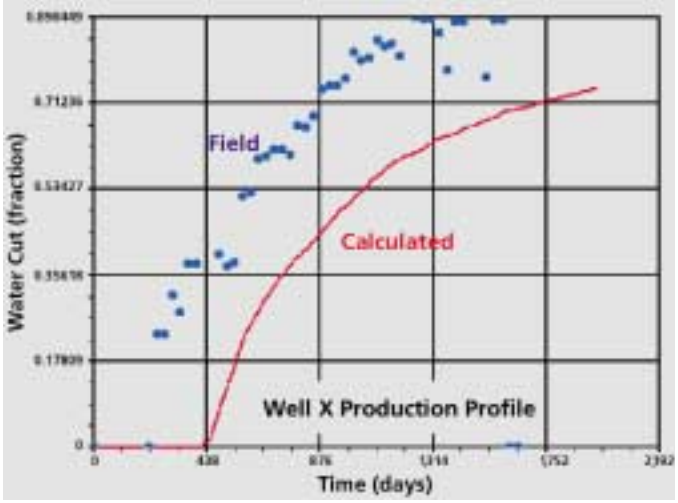

Fig. 24b. Water cut of conventional model. Note the water arrival time compared to field date.

figure shows a very homogeneous porosity distribution, achieved by the inverse distance interpolation using only the well porosity data.

The permeability model was built by directly transforming this porosity model. A regression line was fitted through the cloud of core porosity and permeability values by averaging the distribution of permeability for a given porosity value. This linear relationship was then used to transform the porosity model. The resulting permeability model is unconstrained, with no actual permeabilities at the well locations. Fig. 20 shows the resulting homogenous permeability distribution derived using this technique.

Fluid flow performance

To determine the level of accuracy between the two approaches and the advantage of data integration, fluid flow simulations were run. Several criteria were set to determine the level of accuracy, which included water breakthrough time, CPU time required to history match and fluid flow movement pattern.

The simulation models were constructed using permeability, porosity, depth and cell thickness and petrophysical rock types. No upscaling was done on either set of models to eliminate any inherent errors associated with upscaling. Relative permeability curves and capillary pressure curves were built for each rock type. The global porosity of rock types were split into five bins for simulation modeling as shown in fig. 21. Water injectors were placed at the down-dip ends of the structure while oil producers were placed on the structural high.

Water floods were modeled using a streamline simulator with the porosity and permeability distributions obtained from both the conventional and the integrated approach. Quick-look water flood simulations provided water breakthrough times, fluid front behavior and water cut comparisons. A detailed fluid flow simulation was also carried out using a finite difference simulation technique for both approaches to assess the required CPU time for history matching and pressure and error analysis comparisons.

RESULTS AND DISCUSSION

Each set of models produced very different flow results in terms of water breakthrough times and fluid movement patterns.

In the case of the integrated models, water had a preferred direction through thin zones of high permeability (fig. 22) capturing the stratification of the reservoir model and more closely matching well observations.

By contrast, for the conventional approach the fluid front movement has no preferred direction throughout the model, shown in fig. 23, because the conventional reservoir model is more homogenous compared to the integrated model. The computed water arrival time of the integrated model is a much closer match to the field data than that of the conventional model shown in fig. 24.

The fluid flow simulation results seem to indicate a significant impact on level of accuracy in both history matching time and well performance. Fig. 25 shows the error analysis for each time step for both the conventional and the integrated models. The error at each time step for the integrated model is smaller and more stable than the errors from the conventional non-integrated model. Another advantage of the integrated approach is clearly seen in the improvement of simulation speed for every time step, shown in fig. 26, with as much as 17 percent savings of computational time without changing the properties of the model.

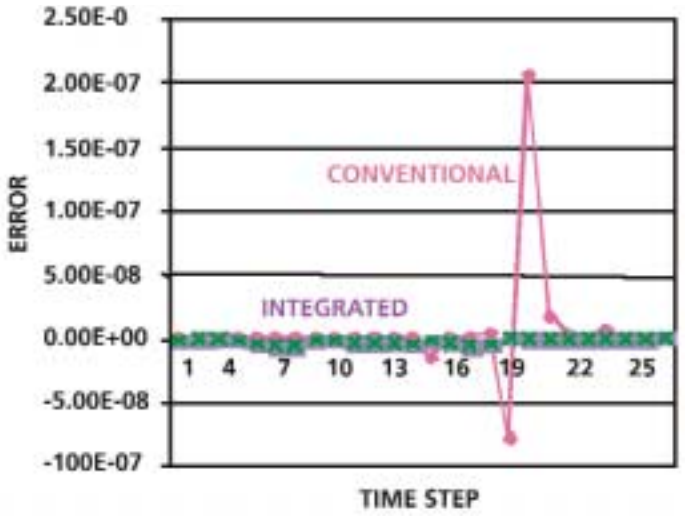

Fig. 25. Error plot analysis for each time step for both approaches

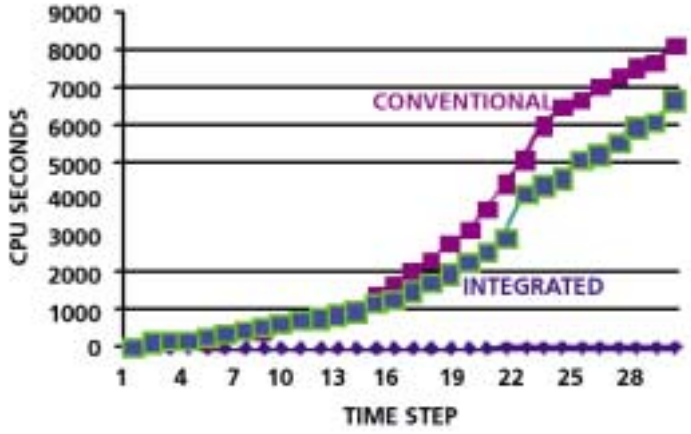

Fig. 26. Comparison of the two approaches in terms of CPU time

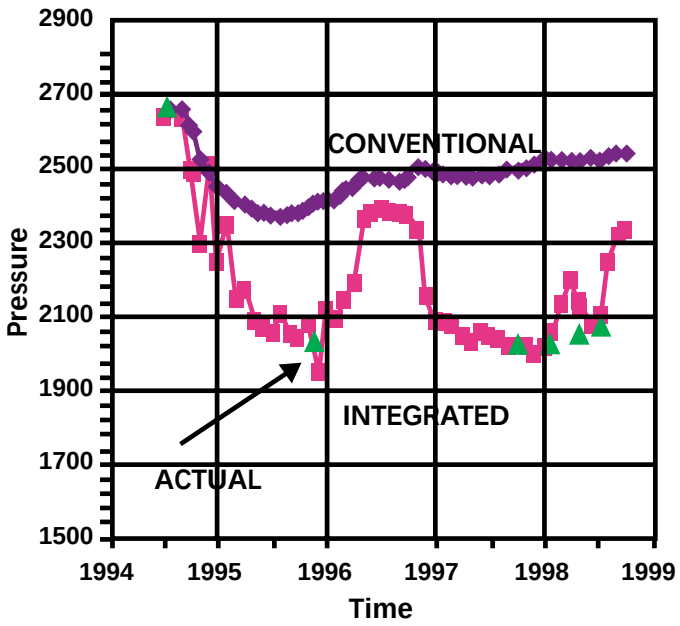

Fig. 27. Pressure match comparison between both types of approaches

Improvement in using the integrated approach is shown in fig. 27, which compares calculated pressure values versus observed pressure. As shown in the figure, the calculated pressures from the integrated model simulation match the observed pressure data. The calculated pressures from the conventional model simulation overestimates the observed pressures by up to 25 percent.

CONCLUSION

A new technique for integrating data of diverse sources and different scales has been presented. The added value of data integration has been demonstrated by the significant effect on the characteristics of the reservoir models generated. The integration of geological depositional facies data produced profound effects on the spatial distribution of petrophysical rock types between wells. Moreover, the incorporation of seismic acoustic impedance data provided additional information allowing the heterogeneity and small-scale variations in the inter-well regions to be captured in the model. The integrated method provided more realistic and meaningful models for the complex heterogeneity of the 'Unayzah reservoir as compared to the homogenous results produced by the non-integrated, conventional approach. The effect of predictions of fluid flow behavior was significant when using the integrated approach. Fluid flow movement patterns, breakthrough time, major reduction of CPU time and the pressure match with observed data are only a few examples of the many advantages of this integrated approach.

ACKNOWLEDGMENTS

The authors would like to extend thanks to the University of Aberdeen for their support. We wish to thank our colleagues Hassan Al-Kaf, Maher Al-Marhoon and Khalid Al-Mashouq for their valuable contributions.

REFERENCES

Al-Ali, Z. and H. Alqassab. 2000. "Optimizing Simulation Models by Upscaling from Integrated Reservoir Models, A Case History," SPE 59448.

Alqassab, H. 1999. "Constraining Permeability Field to Engineering Data: An Innovative Approach in Reservoir Characterization," Saudi Aramco Journal of Technology, fall.

Alqassab, H. and C. Heine. 1998. "A Geostatistical Approach to Attribute Interpolation Using Facies Templates, An Advanced Technique in Reservoir Characterization," SPE 49449.

Araktingi, U. and W. Bashore. 1992. "Effects of Properties in Seismic Data on Reservoir Characterization and Consequent Fluid Flow-Predictions When Integrated With Well Logs," SPE 24753.

Araktingi, U., W. Bashore, T. Hewett and T. Tran. 1990. "Integration of Seismic and Well Log Data in Reservoir Modeling," presented at the Third Annual NIPER Conference on Reservoir Characterization, Tulsa, Oct. 5-7.

Jones, D., Z. Al-Ali. M. Al-Khalifa and Aktas, G. 1999. "Development of a Conceptual Model for The Study Field, Saudi Arabia," an internal report.